An Acid-Responsive Single Trichromatic Luminescent Dye That Provides Pure White-Light Emission

Keigo Imamura,[a] Yoshifumi Ueno,[a] Seiji Akimoto,[a] Kazuo Eda,[a] Yanqing Du,[b] Chaolu Eerdun,[b] Meiling Wang,[b] Kumiko Nishinaka,[a] and Akihiko Tsuda*[a, c]

A novel acid-responsive single trichromatic luminescent dye capable of emitting pure white light (WL) is reported. A newly designed *p*-phenylene-bridged bipyrrole bearing *N*-alkylimino groups (**1a**) specifically provides WL emission upon mixing with trifluoroacetic acid (TFA) in a CH_2Cl_2 solution. The emission originates from the trichromatic luminescent behavior of **1a** upon protonation of the imino groups. The blue-light-emitting **1a** exhibits dramatic color changes in fluorescence to orange and green upon mono- and diprotonation, respectively, providing a wide emission band in the range of $\lambda = 400$–800 nm that provide WL when the compound is in a dynamic equilibrium between the three states. The sample also exhibits low self-absorption of the emitted light and a high fluorescence quantum yield upon excitation with UV light.

Synthesis of colorful luminophoric molecules through artificial design of a π-conjugation system is desirable in organic chemistry. With an objective to utilize them in practical lighting applications, a white-light (WL) luminescent dye, which has little or no light absorption in the visible region and a high fluorescence quantum yield, is especially valuable. WL-emissive materials are generally prepared upon mixing multiple lumino-phores with a delicate balance to cover the wide wavelength range of $\lambda = 400$–800 nm.[1] To simplify the preparation procedures and maintain the original color over long periods of time, synthesis of a molecular luminophore that exhibits WL emission within one single molecular system has been an important research subject.[2,3] Reported examples of WL-emissive single molecular luminophores include independent multilumi-nophoric components in the molecule to give wide emission bands in the visible region. Protonation and host–guest complexation of a single luminophore, whose luminescence color varies with the formation of multiluminophoric species in equilibria, are also known to achieve WL emission.[4,5] To date, however, a single luminescent dye that provides WL emission is still rare. Furthermore, to the best of our knowledge, pure WL emission with International Commission on Illumination (CIE) coordinates (0.33, 0.33) has never been achieved in a single molecular system. In this study, we designed stimuli-responsive bipyrrole derivatives and found that a *p*-phenylene-bridged bi-pyrrole bearing *N*-alkylimino groups **1** becomes an acid-responsive single trichromatic BOG (blue, orange, and green) luminescent dye capable of emitting pure WL in solution.

π-Conjugated bipyrrole derivatives have been reported as luminophores.[6] Their unique optical, electronic, and structural features enable their utilization as dyes, sensors, and optoelectronic devices, and as building blocks in synthesizing macrocycles and supramolecular architectures.[7–13] To develop a color-tunable multichromatic single luminescent dye that is usable for fabricating smart multicolor lighting materials and devices, our strategies include insertion of a spacer unit, attachment of functional groups to the bipyrrole backbone, and control of the π-electronic interactions with external chemical stimuli.

We synthesized imino-substituted bipyrrole derivatives **1**–**4**, containing an aryl or heteroaryl spacer, and an amide-substituted bipyrrole derivative **5** (Scheme 1). Phenylene- or thienyl-bridged bipyrrole derivatives bearing ethoxycarbonyl groups at pyrrolic α positions were synthesized according to procedures reported previously (see the Supporting Information).[14] The ethoxycarbonyl groups were then removed upon treatment with NaOH at high temperature, and subsequent Vilsmeier–Haack reactions with DMF and $POCl_3$ allowed an addition of formyl groups at the same positions. The formyl groups are readily converted into the corresponding imines bearing various functional groups on the nitrogen atom through substitution and elimination reactions with amine in the presence or absence of an acid catalyst (products isolated in yields of 54–86%).

[a]   K. Imamura, Y. Ueno, Prof. Dr. S. Akimoto, Prof. Dr. K. Eda, K. Nishinaka, Prof. Dr. A. Tsuda
      Department of Chemistry
      Graduate School of Science
      Kobe University
      1-1 Rokkodai-cho, Nada-ku
      Kobe 657–8501 (Japan)
      E-mail: tsuda@harbor.kobe-u.ac.jp

[b]   Y. Du, Prof. Dr. C. Eerdun, Prof. M. Wang
      School of Pharmaceutical Sciences
      Inner Mongolia Medical University
      Jinshan Economic & Technology Development District
      Hohhot, Inner Mongolia 010100 (P.R. China)

[c]   Prof. Dr. A. Tsuda
      Department of Chemistry
      Shiga University of Medical Science
      Seta Tsukinowa-cho, Otsu
   Shiga 520–2192 (Japan)
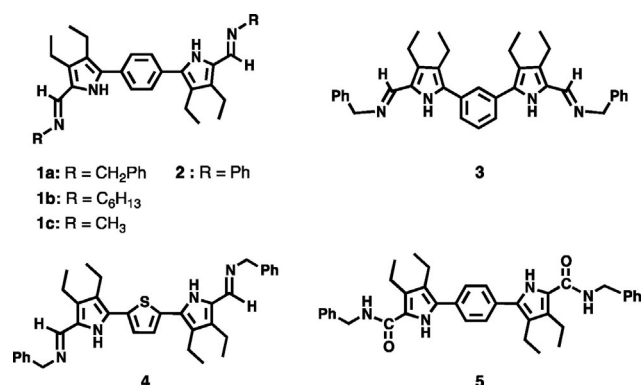
Scheme 1. Imino- or amide-substituted bipyrroles containing a phenylene or thienyl spacer.

We obtained crystals of **1 b** through a vapor diffusion method with chloroform and acetonitrile and the crystals were characterized by means of single-crystal X-ray diffraction analysis (Figure 1; see also Table S1 in the Supporting Information).[15] In the crystal, two pyrrole components adopt a twisted geometry with an *anti*-folded conformation through the phenylene spacer. The dihedral angle of pyrrole and phenylene components is 33.3° on average, indicating steric repulsion between the ethyl group attached to the pyrrole β position and the phenylene ring. The bond length between the aromatic rings (1.47 Å) is consistent with the usual sp^2–sp^2 carbon distance. With respect to the imino group attached to the pyrrole ring, the N1-C1-C2-N2 torsion angle and the C1—C2 bond length are 12.5° and 1.44 Å, respectively, indicating their π conjugation.

We then focused on the strong basicity of the imino groups that conjugate with the pyrrole ring, and on the expected
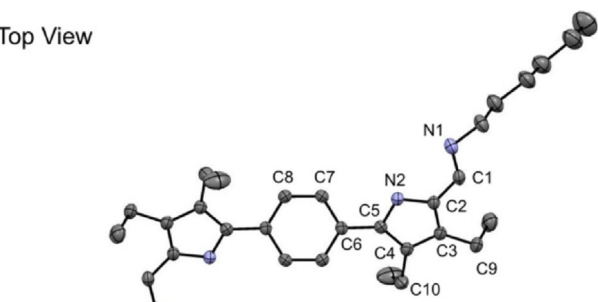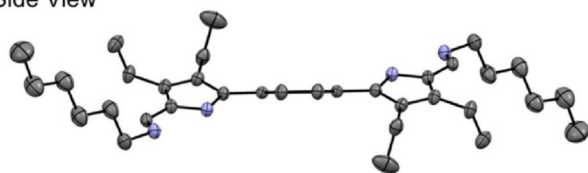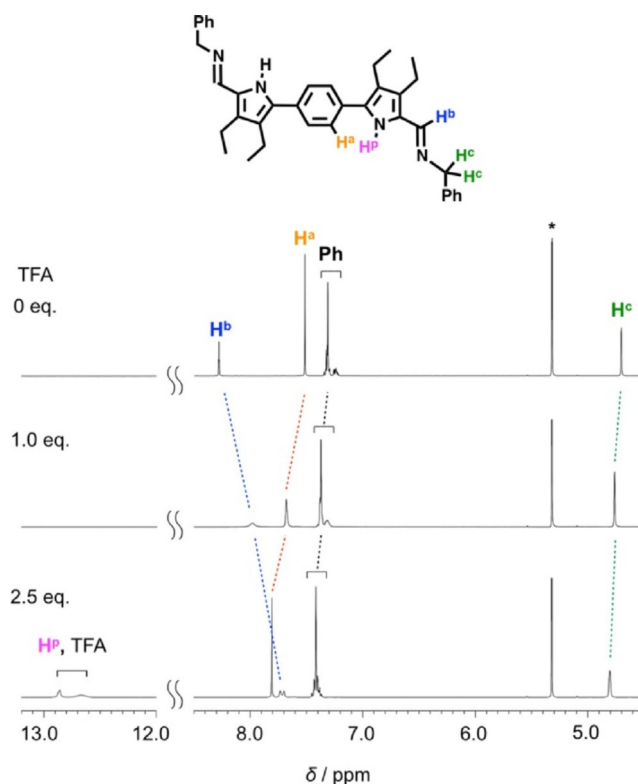
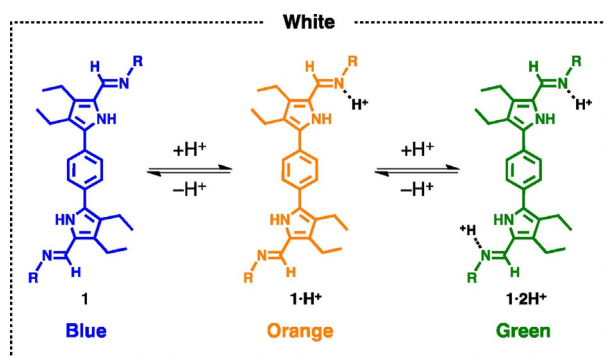changes in the electronic properties of the bipyrrole derivatives through acid–base interactions. As an example, a ¹H NMR spectroscopic titration experiment of a CD_2Cl_2 solution of **1 a** with trifluoroacetic acid (TFA) was demonstrated (Figure 2). Sig-


Figure 2. Changes in the ¹H NMR spectra (400 MHz) of **1 a** upon titration with TFA in CD_2Cl_2 at 20 °C. [**1 a**] = 5.7×10^{-3} M.

nals for singlets at $\delta = 8.28$, 7.51, 4.70 ppm and multiplets at 7.35–7.22 ppm, respectively, corresponding to the imine, phenylene, benzyl, and phenyl protons, were observed (Figure S1). When an equimolar amount of TFA was added into the sample solution, the imine proton was upfield shifted to $\delta = 7.98$ ppm, while the other signals were shifted downfield to 7.68, 4.76, and 7.41–7.29 ppm, respectively. All of the signals, especially for the imine proton, were broadened. These results indicate that one of the imine nitrogens in **1 a** undergoes protonation by TFA in rapid equilibria due to association and dissociation. Further addition of TFA also brought about peak shifts in the same manner, but the peaks became sharp. The observed spectral changes were saturated after an addition of 2.5 equivalents of TFA. At this ratio, the imine proton signal showed splitting, and an additional two signals that likely originate from pyrrole-NH and TFA appeared in the lower magnetic field region. These observed spectral features indicate that **1 a** complexes with TFA mainly at the imino groups to give 1:1 (**1 a·H⁺**) and 1:2 (**1 a·2H⁺**) salts under dynamic equilibria (Scheme 2). Electrospray ionization Fourier transform mass spectrometry (ESI-FT MS) for the 1:1 mixture solution actually showed the presence of both mono- and diprotonated **1 a** (Figure S2).

Figure 1. ORTEP diagram of **1 b**, with ellipsoids set at 50% probability. Hydrogen atoms are omitted for clarity.

Scheme 2. Schematic illustration of white-light emission with an acid-responsive single BOG luminescent bipyrrole.
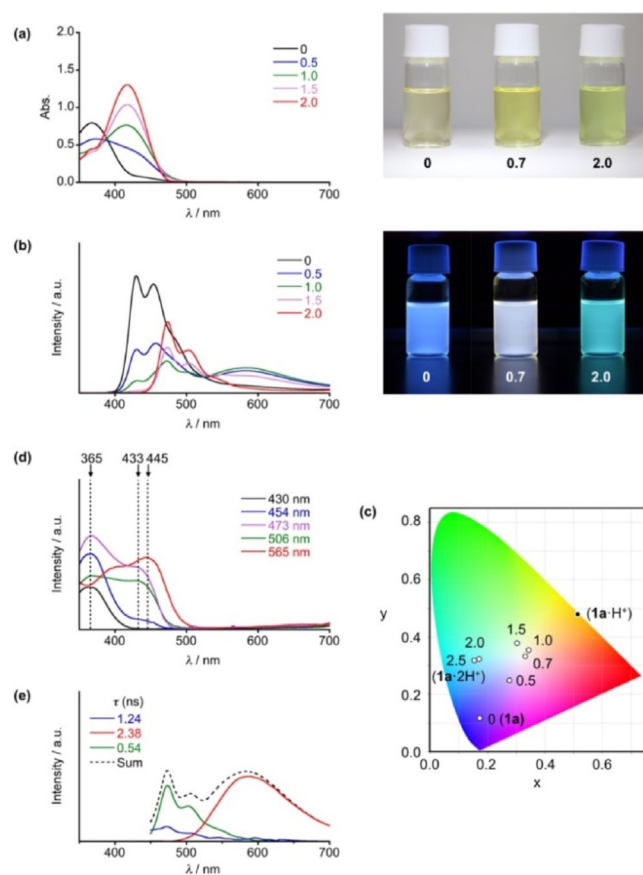
Figure 3. a) UV/Vis absorption spectroscopic titration of bipyrrole **1a** with TFA in CH_2Cl_2 at 20 °C and corresponding photographs, and b) the corresponding steady-state fluorescence spectra upon excitation at 392 nm and corresponding photographs under irradiation with a UV lamp (365 nm). Values (0, 0.5, 1.0 etc) correspond to the number of added equivalents of TFA. c) Emission colors in a CIE 1931 chromaticity diagram. d) Excitation spectra of the 1:1 mixture of **1a** and TFA monitored for the emission bands at 430, 454, 473, 506, and 565 nm. e) Deconvoluted fluorescence spectra of the 1:1 mixture from time-resolved fluorescence spectroscopy. [**1a**] = 2.0×10^{-5} M.

A CH_2Cl_2 solution containing **1a** with a concentration of 2.3×10^{-5} M has a pale-yellow appearance and also exhibits strong blue emission upon photoirradiation with a UV lamp ($\lambda = 365$ nm; Figure 3 a,b). In the UV/Vis absorption and fluo-

rescence spectra, the sample solution exhibited the lowest-energy absorption band at $\lambda_{max} = 368$ nm with a molar absorption coefficient $\varepsilon = 3.46 \times 10^5$ M^{-1}cm^{-1} and emission bands at $\lambda_{max} = 430$ and 454 nm with a fluorescence quantum yield $\Phi_F = 0.53$, respectively. When a CH_2Cl_2 solution of **1a** was titrated with TFA, the absorption band was red-shifted to $\lambda_{max} = 417$ nm, and the observed spectral change was saturated at a 2.0–2.5 equiv of added TFA. The association constants of 1:1 and 1:2 complexation in the CH_2Cl_2 solution at 20 °C were estimated to be $K_1 = 8.5 \times 10^8$ and $K_2 = 3.8 \times 10^7$ M^{-1}, respectively, through curve fitting in the computer simulation of the titration profile. Taking a closer look at the absorption spectra of the 1:1 and 1:2 mixtures, the former is relatively broad, and its band tail extends to 500 nm. The color of the sample solution turned from yellow through to yellow/green. In the fluorescence spectra, dramatic spectral changes were observed in the corresponding titration profile. The 1:1 mixture upon excitation at $\lambda = 392$ nm gave rise to broad emission bands in the range of 400–700 nm with emission maxima at 431, 472 and 581 nm. However, in contrast, the 1:2 mixture provided sharp emission bands at 473 and 502 nm without the lower energy emission band. Their fluorescence quantum yields upon excitation at 375 nm also stayed high, with $\Phi_F = 0.53$ and 0.59 for 1:1 and 1:2 mixtures, respectively. Accordingly, the 1:1 and 1:2 mixtures showed dramatic emission color changes, from blue to green via white. Then, with a careful titration experiment, we found that the pure WL emission at CIE coordinates (0.33, 0.33) was achieved at a ratio of 1:0.7 of **1a** and TFA (Figure 3 c). Polystyrene films of **1a,** and 1:0.3 and 1:2 mixtures of **1a** and TFA also provided blue, yellowish white, and green emissions, respectively (Figure S3).

Fluorescence excitation spectra of the 1:1 mixture of **1a** and TFA monitored for the distinguishable emission bands provided different profiles (Figure 3 d). When the higher energy emission bands at 430 and 454 nm were monitored, the excitation spectral bands mainly appeared at $\lambda_{max} = 365$ nm, which corresponds to the lowest energy absorption band of **1a**. In contrast, red-shifted spectra with a shoulder around 433 nm were observed through monitoring at wavelengths of 473 and 506 nm. The lowest energy emission band at 565 nm provided the more red-shifted excitation spectrum with $\lambda_{max} = 445$ nm and a shoulder around 400 nm. Judging from these excitation spectra and considering together with the titration profiles in absorption and fluorescence spectra, emission bands observed at 430 and 454 nm, 473 and 506 nm, and 565 nm may mainly originate from **1a**, **1a**·2H$^+$, and **1a**·H$^+$, respectively. As support for this consideration, relative band intensities of λ_{max} values in the fluorescence spectrum could also be varied by changing the excitation wavelength (Figure S4).

Time-resolved fluorescence spectroscopy, together with the fluorescence lifetime measurement upon excitation at 408 nm, revealed that the observed fluorescence spectrum of a 1:1 mixture of **1a** and TFA is actually composed of three species with the respective fluorescence lifetimes $\tau = 1.24$, 2.38, and 0.54 ns (Figure S5 and S6). By reference to the steady-state fluorescence spectra of **1a** and the 1:2 mixture of **1a** and TFA, they can be characterized as **1a**, **1a**·H$^+$ and **1a**·2H$^+$, respectively.

Then, spectral deconvolution of the observed fluorescence spectrum of the 1:1 mixture could be demonstrated as shown in Figure 3e. The deconvoluted spectrum clarified that the monoprotonated **1a** provides a single emission band at $\lambda_{max} = 588$ nm, corresponding to an orange color with CIE (x, y) coordinates of (0.51, 0.48), as shown in Figure 3c. Conclusively, the 1:1 mixture of **1a** and TFA yields blue-, orange-, and green-emissive species, originating from **1a**, **1a·H⁺** and **1a·2H⁺**, respectively, in solution (Scheme 2). The relatively longer lifetime of **1a·H⁺** may allow an increase in the fluorescence intensity in the lower energy region in the steady-state fluorescence spectrum so as to achieve WL emission.

The wavelength and intensity of the lowest energy emission band originating from **1a·H⁺** was highly dependent on the solvent (Figure S7), indicating that it can be attributed to an intramolecular charge transfer (CT) emission.[16] The CT may occur from an electron-donating imino group to the electron-accepting protonated group through a π-conjugated phenylene-bridged bipyrrole core. This hypothesis is actually supported by the density functional theory (DFT) calculations at the cam-B3LYP/6-31G level for N-methyl substituted **1c**, and mono- and diprotonated **1c** (Figure 4).[17] The highest occupied molecular
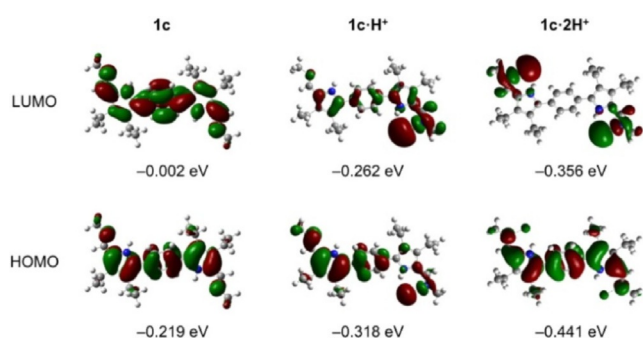

Figure 4. DFT calculations of HOMO (bottom) and LUMO (top) of N-methyl substituted **1c**, **1c·H⁺**, and **1c·2H⁺** with their energies calculated at the cam-B3LYP/6-31G level. Calculations were demonstrated with X-ray crystallographic data of **1b** with an N–H⁺ distance = 2.1 Å.

orbital (HOMO) and lowest unoccupied molecular orbital (LUMO) of **1c** mainly consist of the π and π* systems of the phenylene-bridged bipyrrole backbone. However, in sharp contrast, the HOMO and LUMO of **1c·H⁺** have larger contributions from the unprotonated side of the bipyrrole backbone and the opposite protonated imino group, respectively. Then, **1c·2H⁺** exhibits large contributions from the π-conjugated backbone and two sets of the protonated imino groups in the HOMO and LUMO, respectively. These results suggest that the monoprotonation only allows opposite contributions of the HOMO and LUMO in the molecule to cause the charge transfer upon photoexcitation. The calculated absorption spectral profiles of **1c**, **1c·H⁺**, and **1c·2H⁺** (Figure S8), reflecting these features, reasonably explain the changes detected in the absorption and fluorescence excitation spectra of **1a** upon the addition of TFA in Figure 3a and Figure 3d.

WL emission was also observed with other Brønsted acids such as HCl and HNO₃, and even with organic salts such as

tetra-n-butylammonium chloride and bromide (Figure S9–11). We then investigated structural requirements of the bipyrrole derivatives for acid-responsive luminescence to be possible by modification of the N-substituent groups and the aromatic spacer moiety. N-hexylimine-substituted **1b**, having a higher solubility in organic solvents, showed essentially the same trichromatic luminescent behaviors as **1a**, with relatively lower $\Phi_F = 0.23$ (Figure S12), but N-phenylimine-substituted **2**, having an extended π-conjugation structure, provided an extremely weak red-shifted fluorescence spectrum, with $\Phi_F = 0.01$ (Figure S13). N-benzylamide-substituted **5** weakly binds TFA, and a steady decrease and broadening of the emission bands were observed with an increasing concentration of TFA (Figure S14). m-Phenylene-bridged **3**, a core-modified version of **1a**, provided the lowest energy absorption band at $\lambda_{max} = 334$ nm, indicating weak π-conjugation compared with that of **1a** (Figure S15). **3** showed very weak blue emission, with $\Phi_F = 0.06$, and no notable color changes were observed upon titration with TFA. However, a thienyl-bridged bipyrrole bearing N-benzylimino groups **4** provided trichromatic emission upon titration with TFA, as observed in **1a** and **1b** (Figure 5). It exhibits the lowest energy absorption band at $\lambda_{max} = 404$ nm, which is lower than that of **1a**, and brought about spectral changes in the lower energy region, resulting in color changes from green to orange to yellow (GOY). These results suggest that the BOG (blue, orange, and green) emissions giving pure WL with
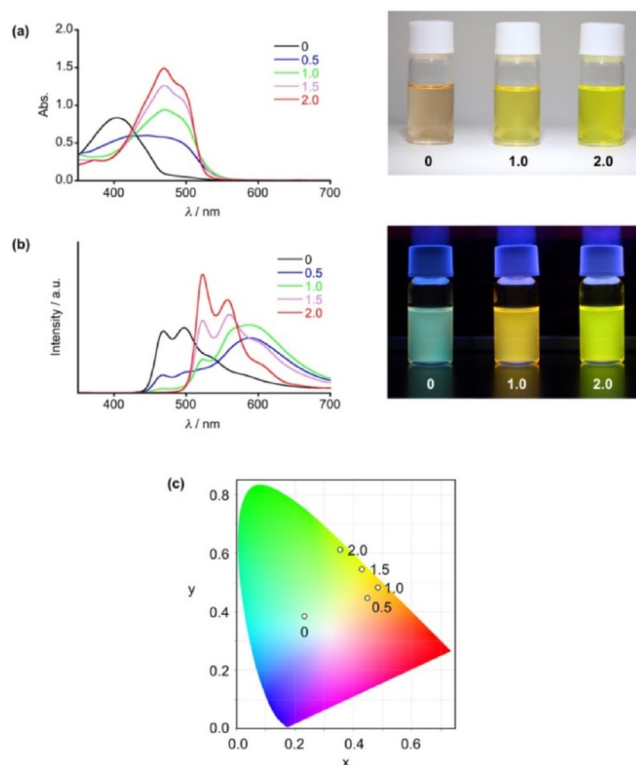
Figure 5. a) UV/Vis absorption spectroscopic titration of bipyrrole **4** with TFA in CH₂Cl₂ at 20 °C and selected corresponding photographs. b) The corresponding steady-state fluorescence spectra upon excitation at 432 nm and corresponding photographs under irradiation with a UV lamp (365 nm). c) Emission colors in a CIE 1931 chromaticity diagram. [**4**] = 2.1 × 10⁻⁵ M.

a high fluorescence quantum yield is a specific property originating from the molecular structure of **1**.

In conclusion, we have successfully synthesized an acid-responsive single trichromatic luminescent dye capable of exhibiting WL emission. *p*-Phenylene-bridged bipyrrole bearing *N*-alkylimino groups **1** provides a blue emission in CH_2Cl_2 solution, but exhibits an orange CT emission and a green emission upon mono- and diprotonation, respectively. Such a stimuli-responsive multichromatic luminophore is advantageous for tuning the emission color at the molecular level. This BOG luminophore could be tuned to exhibit pure WL emission with a high fluorescence quantum yield when mixed with 0.7 equivalents of TFA. These results suggest a new method and provide a rational molecular design for preparing a stimuli-responsive single multichromatic luminescent dye capable of emitting WL. Such smart luminescent dyes could have fascinating uses for a variety of applications, such as inks, paints, cosmetics, sensors, and optoelectronic devices.

Acknowledgements

Conflict of interest

The authors declare no conflict of interest.

[1] a) M. Chen, Y. Zhao, L. Yan, S. Yang, Y. Zhu, I. Murtaza, G. He, H. Meng, W. Huang, *Angew. Chem. Int. Ed.* **2017**, *56*, 722–727; *Angew. Chem.* **2017**, *129*, 740–745; b) S. K. Sarkar, G. R. Kumar, P. Thilagar, *Chem. Commun.* **2016**, *52*, 4175–4178.

[2] a) C.-F. Liu, Y. Jiu, J. Wang, J. Yi, X.-W. Zhang, W.-Y. Lai, W. Huang, *Macromolecules* **2016**, *49*, 2549–2558; b) F. Wang, L. Wang, J. Chen, Y. Cao, *Macromol. Rapid Commun.* **2007**, *28*, 2012–2018.

[3] a) K.-C. Tang, M.-J. Chang, T.-Y. Lin, H.-A. Pan, T.-C. Fang, K.-Y. Chen, W.-Y. Hung, Y.-H. Hsu, P.-T. Chou, *J. Am. Chem. Soc.* **2011**, *133*, 17738–17745; b) S. Park, J. E. Kwon, S. H. Kim, J. Seo, K. Chung, S.-Y. Park, D.-J. Jang, B. M. Medina, J. Gierschner, S. Y. Park, *J. Am. Chem. Soc.* **2009**, *131*, 14043–14049.

[4] A. K. Pati, S. J. Gharpure, A. K. Mishra, *J. Phys. Chem. A* **2016**, *120*, 5838–5847.

[5] a) K. Yamaguchi, T. Murai, J.-D. Guo, T. Sasamori, N. Tokitoh, *ChemistryOpen* **2016**, *5*, 434–438; b) H. V. Huynh, X. He, T. Baumgartner, *Chem. Commun.* **2013**, *49*, 4899–4901.

[6] a) X. Li, G. Ji, Y.-A. Son, *Dyes Pigm.* **2016**, *124*, 232–240; b) T. Okawara, A. Doi, T. Ono, M. Abe, K. Takehara, Y. Hisaeda, S. Matsushima, *Tetrahedron Lett.* **2015**, *56*, 1407–1410; c) C.-M. Che, C.-W. Wan, W.-Z. Lin, W.-Y. Yu, Z.-Y. Zhou, W.-Y. Laic, S.-T. Lee, *Chem. Commun.* **2001**, 721–722.

[7] a) Z. Cai, Y. Guo, S. Yang, Q. Peng, H. Luo, Z. Liu, G. Zhang, Y. Liu, D. Zhang, *Chem. Mater.* **2013**, *25*, 471–478; b) A. Cihaner, O. Mert, A. S. Demir, *Electrochim. Acta* **2009**, *54*, 1333–1338; c) T. Tshibaka, I. U. Roche, S. Dufresne, W. D. Lubell, W. G. Skene, *J. Org. Chem.* **2009**, *74*, 9497–9500.

[8] a) A. Kumar, M. Borgen, L. I. Aluwihare, W. Fenical, *Environ. Sci. Technol.* **2017**, *51*, 589–595; b) K. Haraguchi, Y. Hisamichi, Y. Kotaki, Y. Kato, T. Endo, *Environ. Sci. Technol.* **2009**, *43*, 2288–2294.

[9] C. C. Hughes, C. A. Kauffman, P. R. Jensen, W. Fenical, *J. Org. Chem.* **2010**, *75*, 3240–3250.

[10] a) M. Yamamura, H. Takizawa, T. Nabeshima, *Org. Lett.* **2015**, *17*, 3114–3117; b) S. K. Kim, J. Lee, N. J. Williams, V. M. Lynch, B. P. Hay, B. A. Moyer, J. L. Sessler, *J. Am. Chem. Soc.* **2014**, *136*, 15079–15085; c) V. V. Roznyatovskiy, N. V. Roznyatovskaya, H. Weyrauch, K. Pinkwart, J. Tübke, J. L. Sessler, *J. Org. Chem.* **2010**, *75*, 8355–8362.

[11] a) N. N. Pati, B. S. Kumar, B. Chandra, P. K. Panda, *Eur. J. Org. Chem.* **2017**, 741–745; b) T. Okujima, C. Ando, S. Agrawal, H. Matsumoto, S. Mori, K. Ohara, I. Hisaki, T. Nakae, M. Takase, H. Uno, N. Kobayashi, *J. Am. Chem. Soc.* **2016**, *138*, 7540–7543.

[12] K. Nakamura, N. Yasuda, H. Maeda, *Chem. Commun.* **2016**, *52*, 7157–7160.

[13] a) J.-i. Setsune, *Chem. Rev.* **2017**, *117*, 3044–3101; b) M. Mori, T. Okawa, N. Iizuna, K. Nakayama, J. M. Lintuluoto, J.-i. Setsune, *J. Org. Chem.* **2009**, *74*, 3579–3582; c) J.-i. Setsune, S. Maeda, *J. Am. Chem. Soc.* **2000**, *122*, 12405–12406.

[14] a) J.-i. Setsune, M. Toda, K. Watanabe, P. K. Panda, T. Yoshida, *Tetrahedron Lett.* **2006**, *47*, 7541–7544; b) J.-i. Setsune, M. Toda, T. Yoshida, *Chem. Commun.* **2008**, 1425–1427; c) J.-i. Setsune, M. Toda, T. Yoshida, K. Imamura, K. Watanabe, *Chem. Eur. J.* **2015**, *21*, 12715–12727.

[15] CCDC 1552509 (**1 b**) contains the supplementary crystallographic data for this paper. These data can be obtained free of charge from The Cambridge Crystallographic Data Centre.

[16] a) X. Zhang, Y.-B. Jiang, *Photochem. Photobiol. Sci.* **2011**, *10*, 1791–1796; b) M. Aleksiejew, J. Heldt, J. R. Heldt, *J. Lumin.* **2008**, *128*, 1307–1316.

[17] DFT calculations were carried out using Gaussian 09 Revision A.1. Geometry optimizations were performed with the X-ray crystallographic data of **1 b** for a single molecule in a gas phase.